physica status solidi a
www.pss-a.com
applications and materials science

The role of vacancies in the mobility of dislocations and grain boundaries in magnesium

O. A. Lambri[1], **M. Massot**[2], **W. Riehemann**[3], **E. J. Lucioni**[1], **F. Plazaola**[2], and **J. A. García**[4]

[1] Facultad de Ciencias Exactas, Ingeniería y Agrimensura, Instituto de Física Rosario, Universidad Nacional de Rosario – CONICET, Escuela de Ingeniería Eléctrica, Laboratorio de Materiales, Avda. Pellegrini 250, 2000 Rosario, Argentina
[2] Elektrika eta Elektronika Saila, Zientzia eta Teknologia Fakultatea, Euskal Herriko Unibertsitatea, P.K. 644, 48080 Bilbao, Spain
[3] Institute of Materials Science and Technology, Clausthal University of Technology, Agricolastraße 6, 38678 Clausthal-Zellerfeld, Germany
[4] Departamento de Física Aplicada II, Facultad de Ciencias y Tecnología, Universidad del País Vasco, Apdo. 644, 48080 Bilbao, Spain

Received 15 July 2006, revised 8 November 2006, accepted 12 December 2006
Published online 9 February 2007

PACS 61.72.Lk, 61.72.Mm, 62.40.+i, 78.70.Bj

Dedicated to Professor P. Lukáč on his 72nd birthday

Vacancy flux or supersaturation enhances grain-boundary mobility, but experimental evidence is not large and in many cases the role of vacancies is only inferred indirectly. We will show effectively in the present work the importance of the vacancy role in grain-boundary mobility in commercial pure and high-purity magnesium using mechanical spectroscopy, electrical resistivity and positron annihilation spectroscopy. It has been found that the mobility decrease of grain boundaries and dislocations is related to vacancy concentration reduction attained after the homogenisation treatment. Indeed, the largest vacancy concentration reduction is observed between 420 and 500 K. Unlocking grain boundaries and dislocations requires new vacancies, generated at temperatures above 500 K. In addition, a new damping peak related to vacancies was discovered at 490 K for an oscillating frequency of 1 Hz.

phys. stat. sol. (a) **204**, No. 4, 1077–1092 (2007) / **DOI** 10.1002/pssa.200622336

Original Paper

phys. stat. sol. (a) **204**, No. 4, 1077–1092 (2007) / **DOI** 10.1002/pssa.200622336

The role of vacancies in the mobility of dislocations and grain boundaries in magnesium

O. A. Lambri[*, 1], **M. Massot**[2], **W. Riehemann**[3], **E. J. Lucioni**[1], **F. Plazaola**[2], and **J. A. García**[4]

[1] Facultad de Ciencias Exactas, Ingeniería y Agrimensura, Instituto de Física Rosario, Universidad Nacional de Rosario – CONICET, Escuela de Ingeniería Eléctrica, Laboratorio de Materiales, Avda. Pellegrini 250, 2000 Rosario, Argentina
[2] Elektrika eta Elektronika Saila, Zientzia eta Teknologia Fakultatea, Euskal Herriko Unibertsitatea, P.K. 644, 48080 Bilbao, Spain
[3] Institute of Materials Science and Technology, Clausthal University of Technology, Agricolastraße 6, 38678 Clausthal-Zellerfeld, Germany
[4] Departamento de Física Aplicada II, Facultad de Ciencias y Tecnología, Universidad del País Vasco, Apdo. 644, 48080 Bilbao, Spain

Received 15 July 2006, revised 8 November 2006, accepted 12 December 2006
Published online 9 February 2007

PACS 61.72.Lk, 61.72.Mm, 62.40.+i, 78.70.Bj

Dedicated to Professor P. Lukáč on his 72nd birthday

Vacancy flux or supersaturation enhances grain-boundary mobility, but experimental evidence is not large and in many cases the role of vacancies is only inferred indirectly. We will show effectively in the present work the importance of the vacancy role in grain-boundary mobility in commercial pure and high-purity magnesium using mechanical spectroscopy, electrical resistivity and positron annihilation spectroscopy. It has been found that the mobility decrease of grain boundaries and dislocations is related to vacancy concentration reduction attained after the homogenisation treatment. Indeed, the largest vacancy concentration reduction is observed between 420 and 500 K. Unlocking grain boundaries and dislocations requires new vacancies, generated at temperatures above 500 K. In addition, a new damping peak related to vacancies was discovered at 490 K for an oscillating frequency of 1 Hz.

1 Introduction

We have reported recently several papers related to the study of the precipitation process in WE43 (Mg – 4 wt% Y – 3.4 wt% Nd – 0.7 wt% Zr), AZ91 (Mg – 9.5 wt% Al – 0.6 wt% Zn – 0.2 wt% Mn) and QE22 (Mg – 2 wt% Ag – 2 wt% Nd–Zr) magnesium alloys [1–3]. Precipitation processes were studied within the temperature range 400–600 K in the following two ways: (a) studying the effects on the damping spectrum caused by the appearance of a precipitation peak and (b) studying the effect of the precipitation process using grain-boundary mobility. In addition, several works have been reported on the damping response of magnesium related to grain-boundary and dislocation mobility within the range of medium homologue temperatures (T/T_m, where T_m is the melting temperature) [4–6]. Besides, an unexpected decrease in the damping at around 420 K annealing temperature was reported and was related to the interaction of impurities with dislocations [6].

[*] Corresponding author: e-mail: olambri@fceia.unr.edu.ar, Phone: +54 341 480 2649, Fax: +54 341 480 2654

The mechanical spectroscopy (MS) technique (mechanical damping and elastic modulus measurements versus temperature) is very sensitive to the microstructure of the sample and therefore quite suitable for the study of lattice defects and their interaction processes in materials. Damping, Q^{-1}, is often produced by the presence of a defect, which causes a local strain coupling to an externally applied stress. It is related to the ratio between the vibrational energy loss and the vibrational energy per cycle. In addition, the elastic modulus is proportional to the square of the natural oscillation frequency, f [4, 7].

Electrical resistivity (ER) measurements are very sensitive to the microstructure, too. Its behaviour is controlled by the competition of two effects: (a) the depletion of impurities from the solid solution and (b) the appearance of internal stresses. In fact, the appearance of internal stresses produces the modification of the interatomic distances leading to a change in the Fermi energy. The band structure can also change during the appearance of internal stresses. Consequently, the coupling with other techniques is mandatory to distinguish which is the physical mechanism controlling the ER behaviour [8, 9].

Positron annihilation spectroscopy (PAS) is a well-established highly sensitive technique for detecting open-volume sites in solids [10]. After the implantation of positrons emitted by a β^+ source (like Na^{22}) in matter, they react with electrons (their anti-particles). When a positron is trapped, annihilation takes place with the characteristics determined by the local electron density, which is lower in the open-volume defect than in the bulk. The reduced electron density implies a reduced annihilation rate. Thus, trapped positrons survive for more time in comparison to the free ones [11]. Trapping is the reason of the great sensitivity of positrons to defects. In fact, if the metal contains defects as vacancies, vacancy clusters and dislocations, i.e. regions of less than average electron density, positrons may become trapped at these defects [12–14].

In the case of Mg, positron lifetime measurements have been performed in well-annealed and electron-irradiated Mg. Indeed, a survey of the various factors, which govern the trapping efficiency in vacancies, leads to the conclusion that magnesium is a borderline case. In the periodic table of elements magnesium is situated between sodium, which is a typical alkali metal showing no trapping at vacancies, and aluminium, in which the positron lifetime increase with respect to the bulk lifetime (well-annealed sample) is about 35%. Indeed, the monovacancy positron lifetime reported in those measurements, 255 ± 5 ps, is about 15% larger than the positron bulk lifetime, 225 ps [15].

In the present work we study grain-boundary and dislocation mobility within the temperature range room temperature (RT)–600 K, in commercial pure and high-purity magnesium, using mechanical spectroscopy, electrical resistivity and positron annihilation spectroscopy. The knowledge of grain-boundary and dislocation mobility mechanisms within this temperature range is important due to the overlapping of precipitation processes that appear in alloyed magnesium, as was shown in the above-cited works.

The present results allow concluding that the mobilities (between RT and 600 K) of both grain boundaries and dislocations in magnesium are controlled by vacancy concentration. In fact, as was already pointed out by Humphreys and Hatherly [16], the vacancy flux or supersaturation enhances the grain-boundary mobility, but the experimental evidence for this is not extensive and in many cases the role of vacancies is only inferred from indirect evidence.

We will show in the present work the importance of the vacancy role in grain-boundary mobility. In addition, a new damping peak related to vacancy interaction is reported.

2 Experimental procedure

The studied samples were obtained from commercial pure (cpMg: 99.8 wt%) and high-purity (hpMg: 99.99 wt%) magnesium cast bars, provided by Magnesium Electron, Manchester, UK. The chemical compositions of the employed specimens, determined by spark emission spectroscopy, are listed in Table 1.

Homogenisation treatment was performed in order to relieve mechanical stresses produced by the machining of the samples and for fixing the starting thermodynamical state of each sample previous to all the subsequent tests, i.e. the same dislocation density, grain size and vacancy concentration. In addition, in the case of homogenised cpMg samples impurity aggregates can be dissolved by means of the

Table 1 Chemical composition of the employed magnesium samples in parts per million.

	Si	Mn	Fe	Ni	Al	Cu	Zn
cpMg (99.8 wt%)	980	737	120	48	38	75	60
hpMg (99.99 wt%)	111	176	286	54	93	13	2

homogenisation treatment. Homogenisation treatments were performed under argon atmosphere at standard pressure, at 823 K during 1 h followed by quenching into RT water.

MS measurements were carried out employing an inverted torsion pendulum which can work at resonant frequencies between 0.2 and 40 Hz for free-decaying vibrations [17, 18]. The oscillations were recorded with an optical system involving a mirror and a photodiode. Measurements were carried out under argon atmosphere at standard pressure. The device is driven automatically by means of a closed-loop computer-controlled setup. For all these measurements the same initial and final values of the decaying amplitudes were used, in order to eliminate possible distortions due to amplitude-dependent damping effects [18]. The samples used in the MS tests were bars of rectangular section (1 mm × 2.2 mm × 20 mm). The maximum strain on the surface of the sample was 5×10^{-5}. Damping and elastic modulus error was less than 2%. MS measurements were performed following subsequent heating and cooling runs on each sample. The final temperature of each heating run was increased by about 30 K, starting from 420 K up to the homogenisation temperature (823 K).

In each thermal cycle the furnace of the pendulum is removed and simultaneously an argon flux is opened in the environment of the sample. The cooling run can be considered to consist of two cooling stages, due to the high thermal inertia of the system for temperatures close to RT. The first involves cooling from the highest temperature reached during the cycles down to 400 K and the second is from 400 K down to RT. The average cooling rates were 14 and 3 K/min, respectively.

Samples, which were heated during the MS tests directly to various final temperatures, were also measured, i.e. without increasing the maximum temperature of each thermal cycle. Besides, MS measurements were also performed at RT, after heating the sample at a rate of 1 K/min up to different final temperatures, under argon at atmospheric pressure, followed by quenching into water at RT. The samples measured under this condition will be called "samples measured under isochronal annealing", in contrast to the samples measured during the thermal cycles which are performed in continuous heating. A summary of the status of measured cpMg samples by means of MS tests is shown in Table 2.

ER measurements were performed at RT by evaluating the eddy-current decay induced in the sample by changing the applied magnetic field [19]. The employed samples were cylinders of 10 mm diameter and 25 mm length. ER values as a function of temperature were measured at RT after heating the sample at a rate of 1 K/min up to various final temperatures, under argon at atmospheric pressure; followed by quenching into RT water.

At least two samples in the same thermal state were employed in each one of the MS and ER tests for checking the reproducibility of the measurements.

Positron lifetime measurements were performed by a conventional fast–fast timing coincidence system. Taken into account the proximity of the average lifetime values in all the measured samples, we performed large statistical measurements where the total number of counts in each measurement was above 2×10^6 counts. The resolution function was approximated by a Gaussian having a FWHM of 240 ps. A ^{22}NaCl source of about 25 μCi contained in an envelope made from a thin Kapton foil (1.1 mg cm^{-2}) was sandwiched in between two samples. The lifetime spectra were analysed with the computer program POSITRONFIT [20]. The source corrections were obtained after measuring very pure (5N) and well-annealed Al and Mg samples. In order to extract the correct source correction, one lifetime was fixed to 382 ps, i.e. the value currently assigned to the Kapton foil [21]. To obtain satisfactory fits a very long component of about 1.5 ns and with low intensity originating very probably from surface effects was needed. The source correction obtained and used in the measurements performed in the Mg samples under study in this work were 382 ps (10.5%) and 1.5 ns (1.5%). After subtraction of the source

Table 2 Status of the cpMg samples employed in the MS tests. Test denomination: A–B–C, where A indicates the sample number, B the heating run number and C the maximum temperature reached in the thermal cycle.

sample denomination	test denomination	heating run #	maximum temperature achieved during the heating (K)	heating mode during the MS tests	state of the sample previous to the MS test
1	1-01-420 K	01	420	continuous	homogenised 823 K,
1	1-02-450 K	02	450	heating	3600 s
1	1-03-470 K	03	470		
1	1-04-506 K	04	506		
1	1-05-540 K	05	540		
1	1-06-570 K	06	570		
1	1-07-590 K	07	590		
1	1-08-600 K	08	600		
1	1-09-620 K	09	620		
1	1-10-640 K	10	640		
1	1-11-658 K	11	658		
1	1-12-690 K	12	690		
2	2-01-430 K	01	430	continuous	deformed in torsion 6%
2	2-02-540 K	02	540	heating	at RT after
2	2-03-550 K	03	550		1-12-690 K test
3	3-01-560 K	01	560	continuous	homogenised 823 K,
3	3-02-560 K	02	560	heating	3600 s
3	3-03-690 K	03	690		
3	3-04-690 K	04	690		
4			370	isochronal	homogenised 823 K,
4			390	annealing	3600 s
4			400		
4			420		
4			450		
4			480		
4			510		

contribution only one component gave satisfactory fits to the spectra. In Figs. 7 and 8 each positron lifetime value represents the arithmetic mean of three measurements. In all the cases the deviation between the three measurements was within the error of the average positron lifetime, amounting to 0.5 ps.

Samples employed in the PAS study were measured at RT after heating the samples at a rate of 1 K/min up to various final temperatures, under argon at atmospheric pressure, followed by quenching into water at RT.

Transmission electron microscopy (TEM) studies were performed in CM 200 transmission electron microscope (Philips, Eindhoven, Netherlands, 200 kV) equipment. Samples were thinned electrolytically using 20% perchloric acid in ethanol at 253 K.

3 Results

3.1 Light and transmission electron microscopy studies

The grain size and grain arrangement were similar in all tested samples detailed in Table 2, i.e. changes in the size or in the shape of the grains were not observed, neither after plastic deformation nor after

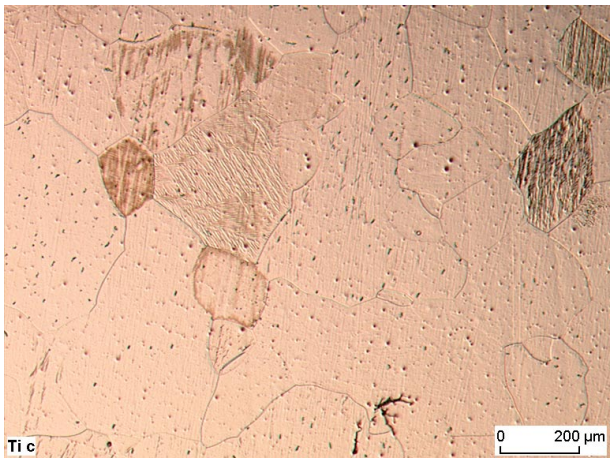

Fig. 1 (online colour at: www.pss-a.com) Optical microscopy photograph of a homogenised cpMg sample.

mechanical spectroscopy tests. Figure 1 shows a photograph of a homogenised cpMg sample where some twins can be observed.

Figure 2 shows a TEM micrograph of a plastically deformed sample (6% torsion) after a 1-12-690 K test. The dislocation density was determined for a homogenised sample, for a sample after the 1-12-690 K test and for the previously cited deformed sample. The measured values were respectively 1×10^{8} cm^{-2}, 8×10^{7} cm^{-2} and 1×10^{11} cm^{-2}. The low dislocation density values measured in the present work are in agreement with previously reported works [4, 22].

3.2 Mechanical spectroscopy studies

Figure 3a shows the measured damping of a homogenised cpMg sample as a function of temperature, during different heating runs, up to successively increasing maximum temperatures, see Table 2. Only heating runs #1, 2, 3, 4, 5, 6, 8 and 12 were plotted in the figure for clarity. In order to have a detailed view of the behaviour of the damping curves at values smaller than 14×10^{-3}, Fig. 3b shows a zoom of

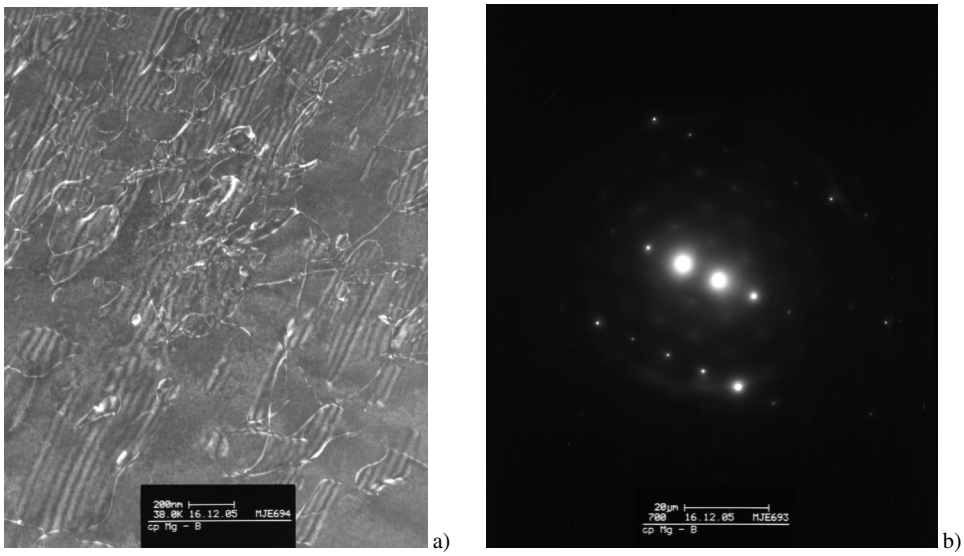

a) b)

Fig. 2 (a) TEM micrograph of a sample plastically deformed after test 1-12-690 K. (b) The diffraction diagram indicating the plane for viewing the microstructure of (a).

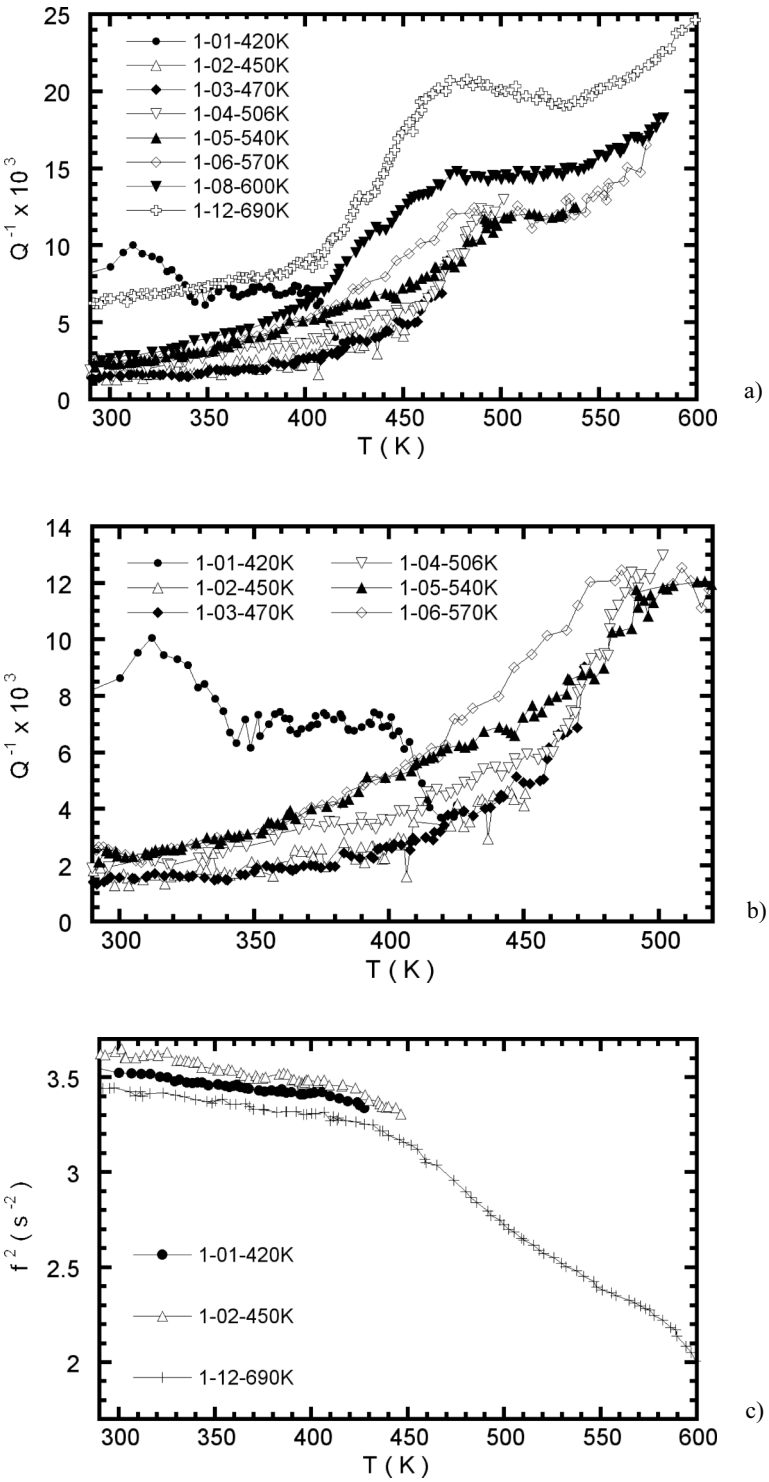

Fig. 3 (a) Damping of homogenised commercial purity magnesium measured during heating. Legends as indicated in Table 2. (b) Zoom of (a) for values of damping smaller than 14×10^{-3}. (c) Elastic modulus (αf^2) for three different heating runs in cpMg. Legends are defined as in Table 2.

the 300–520 K range for runs #1 to 6. The sample was vibrating during the cooling, but the damping was measured only in the small cooling rate zone close to RT, because of the high cooling rate at higher temperatures. As can be seen from the figure, the first run-up in temperature shows a small damping peak at around 320 K. At higher temperatures the damping curve does not change up to around 400 K and subsequently it decreases at around 420 K (see Fig. 3b). Damping values corresponding to the first cooling are completely overlapped by damping points measured during heating run #2. In addition, an increase in temperature to 470 K during run-up #3 does not produce clear changes in the damping spectrum.

In contrast, during run-up #4, a slight damping increase started to appear at around 350 K. Moreover, a peak seems to appear at around 490 K. Even if changes in the spectrum of run-up #4 are small these changes have also been found in two other samples with the same thermal history.

After annealing up to 540 K, during run-up #5, the damping spectrum of run-up #6 shows a damping peak at around 480 K, which could be composed of more than one elementary damping peak. In addition, the damping peak height at 480 K increases as the final temperature of each cycle increases (Fig. 3a).

Heating the sample to 658 K leads to a strong increase of the background damping (see curve 1-12-690 K in Fig. 3a).

It should be stressed that during the heating runs, up to temperatures lower than 500 K, the characteristic grain boundary damping peak of magnesium, which usually appears at temperatures of about 420 K (at 1 Hz), did not appear. In contrast, a peak at approximately 480 K develops.

Frequency squared (proportional to the elastic modulus) versus temperature is plotted in Fig. 3c, for heating runs #1, 2 and 12. For clarity only three curves have been plotted; however, they summarise the behaviour of the elastic modulus during the 12 heating and cooling runs. As can be seen from the figure, the elastic modulus during the second run-up is higher than the corresponding value for the homogenised sample. In addition, the modulus remained higher than the values of the homogenised sample up to an annealing temperature of 500 K. During the successive heating runs, up to temperatures higher than 500 K, the elastic modulus began to decrease progressively, reaching the smallest values during run-up #12.

Figure 4 shows the damping spectra of samples of type #2, plastically deformed in situ under a maximum torsion of 6% at room temperature. The deformation process was carried out after the test 1-12-690 K (see Table 2 and Fig. 3a). As can be seen from the figure a damping peak at 320 K has again developed, followed by a damping jump down at around 420 K. In addition, the background of all curves is higher

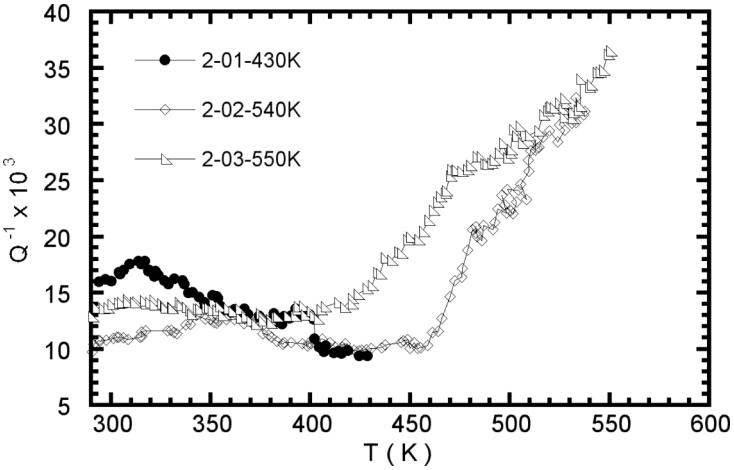

Fig. 4 Damping of "in situ" plastically deformed cpMg sample (6% in torsion) at room temperature after heating run 1-12-690 K of Fig. 3a, see Table 2.

than for sample #1, due to the large quantity of free dislocations produced by the deformation process. During the second run-up, the damping does not change very much up to around 450 K. Besides, the characteristic grain-boundary relaxation at around 420 K does not develop. Nevertheless, the appearance of a relaxation peak at higher temperatures (490 K) can be observed. In addition, in the run-up #3, after annealing up to 540 K (during run-up #2), a wide damping peak develops between RT and 550 K, which is composed by more than one elementary peak.

The damping spectra in deformed samples exhibit a wide peak between RT and 550 K, in similar mode as for the homogenised samples. However, the following different features should be highlighted: (a) the damping background is larger in deformed samples, about twice, and (b) the peak height of the damping peak at about 490 K is larger in deformed samples than in homogenised ones, when the same temperature is reached in the previous annealing. This last difference will be shown more clearly in the next paragraphs and figures.

Furthermore, damping and elastic modulus measurements performed on a homogenised sample #3 (see Table 2), which was thermally cycled with different final temperatures than the ones plotted in

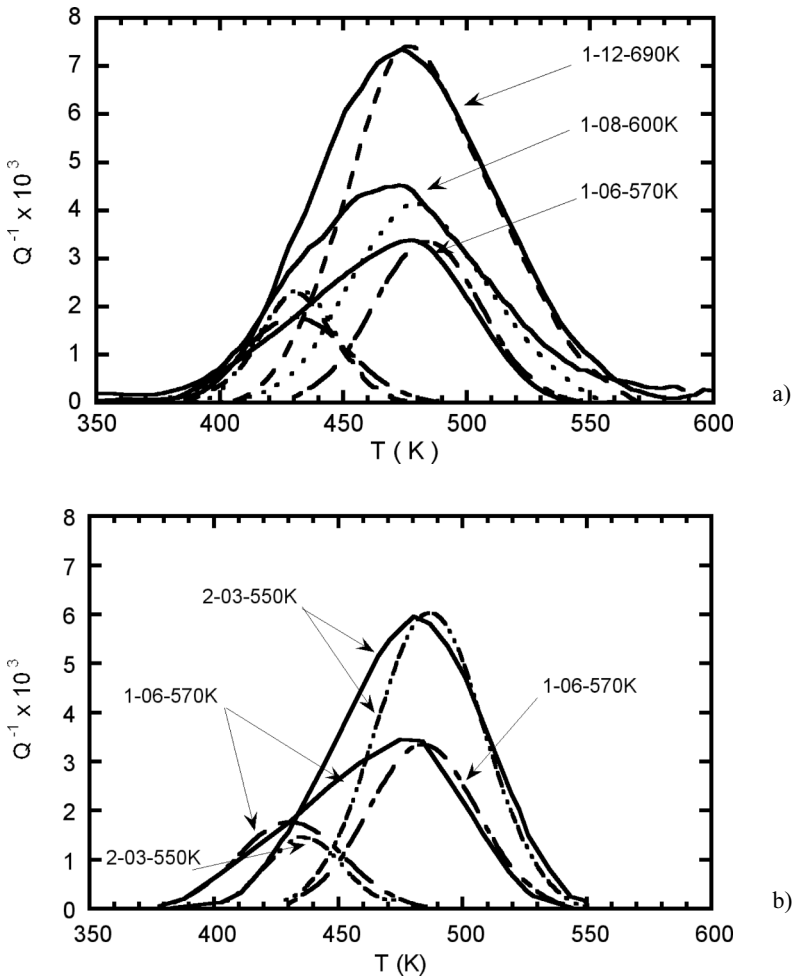

Fig. 5 (a) Alt-dashed, dotted and dashed lines represent the deconvoluted peaks for spectra 1-06-570 K, 1-08-600 K and 1-12-690 K after background subtraction (full lines) of Fig. 3a. (b) Deconvoluted peaks for the spectra 1-06-570 K and 2-03-550 K, corresponding to homogenised and plastically deformed samples, respectively, previously heated up to 540 K. Full lines are spectra after background subtraction.

Fig. 3, exhibited the same behaviour as #1 type samples. In fact, the characteristic of the damping and elastic modulus spectra depends on the previous annealing temperature, which is reached in the previous temperature run-up. In addition, sample #4, which was measured at RT under an isochronal annealing condition, exhibits a similar damping response to the one shown in Fig. 3a, which is also in agreement with previous works.

In Fig. 3a the plotted damping spectra show a clear damping peak within the temperature range 380–550 K (1-06-570 K, 1-08-600 K and 1-12-690 K tests). In fact, firstly, run-up #4 (1-04-506 K) begins to reveal the appearance of a peak at higher temperatures (about 490 K). In the next heating run the peak at around 490 K becomes more evident and another peak at lower temperature can also be observed. Moreover, during run-up #8 (1-08-600 K) a clear hump over the low-temperature tail of the damping peak is present. This suggests that the peak is composed by more than one elementary peak. Consequently, the whole peak was deconvoluted.

Figure 5a shows the three damping peaks, after background subtraction, corresponding to heating runs #6, 8 and 12 of Fig. 3a (1-06-570 K, 1-08-600 K and 1-12-690 K spectra), plotted by full lines. Peak Fit V.4 [23] performed the background subtraction with cubic polynomials. Deconvolution of the spectra was also performed by means of Peak Fit using the second-derivative method with Gaussian functions. Owing to the background subtractions and the subsequent deconvolution the error bandwidth related to damping is less than 0.7×10^{-3} in the plotted curves of Fig. 5.

The alt-dashed, dotted and dashed lines indicate the deconvoluted peaks for 1-06-570 K, 1-08-600 K and 1-12-690 K curves, respectively. The deconvoluted damping peak at lower temperatures would increase slightly its peak height up to run-up #8. From run-ups #8 to 12, the peak height stabilises. In contrast, the peak at higher temperatures increases as the final temperature of the thermal cycles increases.

Figure 5b makes it easy to highlight the effects of the plastic deformation on the relaxation peaks. It shows the damping peaks (full lines) after background subtraction for previously homogenised (1-06-570 K) and plastically deformed (2-03-550 K) samples. The samples were annealed in the previous heating run, up to the same maximum temperature, 540 K (see Table 2). As can be seen from the figure the peak height for the maximum at around 490 K is larger in the deformed sample than in the homogenised one, about two times larger indeed. In addition, the peak at 430 K in the deformed sample is slightly smaller than in the homogenised one.

On the other hand, in order to obtain the activation energy for both relaxation peaks, the natural oscillating frequency f was changed by about one order of magnitude from about 0.5 Hz up to around 5 Hz. Three different oscillating frequencies were employed. Figure 6 shows the corresponding Arrhenius plots

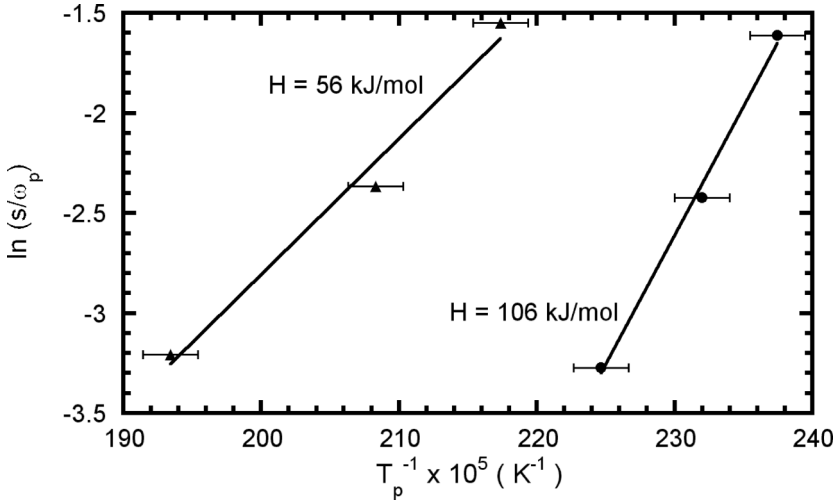

Fig. 6 Arrhenius plots for the grain-boundary and vacancy peaks.

for the deconvoluted peaks, where $\omega = 2\pi f$ and the subscript p indicates values corresponding to circular frequency and temperature at the maximum damping value.

The calculated activation energy for the lower-temperature peak is 106 kJ/mol (1.11 eV), while for the higher-temperature peak the activation energy is 56 kJ/mol (0.59 eV). The activation energy for the relaxation peak at lower temperatures is close to the self-diffusion value for magnesium (134 kJ/mol – 1.4 eV – [24, 25]). In contrast, the activation energy calculated for the higher-temperature peak is smaller than the self-diffusion value. Indeed, it is close to the values for the formation and migration of vacancies [24].

Error bars in the temperature axis show the largest uncertainty due to the background subtraction and peak deconvolution procedure. The error is lower than 10 K, giving rise to the following activation energy intervals for each peak. Low-temperature peak: 156 kJ/mol (1.64 eV) ≥ 106 kJ/mol (1.11 eV) ≥ 80.4 kJ/mol (0.84 eV). High-temperature peak: 66 kJ/mol (0.69 eV) ≥ 56 kJ/mol (0.59 eV) ≥ 48.81 kJ/mol (0.51 eV). In comparison, the error in frequency can be neglected.

3.3 Electrical resistivity and positron annihilation spectroscopy studies

Figure 7 shows the behaviour of the ER measured for a homogenised cpMg sample at RT as a function of annealing temperature. As can be seen from the figure, the curve exhibits firstly an increase up to about 350 K followed by a decrease at approximately 420 K. At higher temperatures up to 500 K the ER increases and, subsequently, it begins to decrease again.

It is interesting to note the good correlation between the changes in the ER curve and the most salient features of the thermal cycles plotted in Fig. 3. In fact, annealing up to temperatures of about 400 K leads to the damping peak at 320 K followed by the constant damping behaviour and the ER curve increase. Annealing up to 420 K develops the jump down in the damping spectrum and the ER curve decrease. After the sample was heated up to around 540 K, both the peak at 490 K and the peak at lower temperature develop and the ER curve reaches its maximum value. Finally, after heating over 540 K, the damping spectra show clearly a wide peak at around 450 K and an increased damping background. Then, the ER curve decreases again.

Also shown in Fig. 7 are the positron average lifetime values measured by PAS. The positron lifetime exhibits a most remarkable behaviour as a function of temperature. In fact, a minimum in the 420–500 K range can be observed.

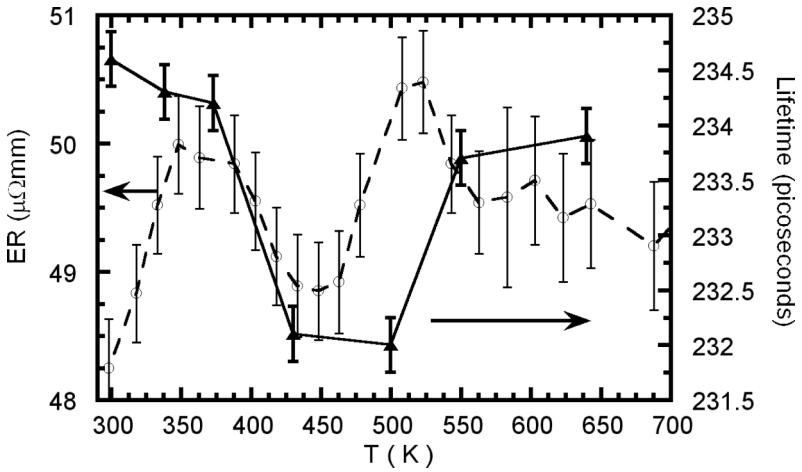

Fig. 7 Electrical resistivity and positron average lifetime in cpMg sample measured at room temperature as a function of the annealing temperature.

Positron lifetime reported in well-annealed (bulk) Mg amounts to 225 ps [15]. The lifetime of positrons trapped at monovacancies produced by electron irradiation is 255 ± 5 ps [15]. Therefore, an average lifetime of 225 ps indicates that all the positrons are annihilating in the perfect Mg structure; however, a value of about 255 ps would indicate that all the positrons are annihilating at monovacancies. Consequently, the average lifetime variation obtained in this work, even if not large, clearly indicates a noticeable variation in the vacancy concentration in the measured samples, particularly with respect to the sample that presents the minimum in the average lifetime.

Figure 8 shows the behaviour of damping and ER measured in a homogenised sample of hpMg. It shows during the first heating run (hp-1-01 test) a damping peak at around 320 K and, subsequently, at around 420 K, a strong decrease of the damping. The damping curve during cooling, after the first heating, coincides with the damping of the next run-up in temperatures during thermal cycles up to about 550 K (hp-1-03 test). In fact, as can be seen from the figure, the full circles of run-up #1, during cooling, are overlapped by the triangles of the hp-1-03 test.

During run-up #3, the appearance of the grain boundary damping peak is not yet clear. In contrast, a peak can be observed at approximately 490 K. In addition, after annealing the sample at higher temperature during the thermal cycles, the grain-boundary peak was restored. Consequently, the damping behaviour of high-purity magnesium is similar to the one of commercial pure magnesium.

The ER curve measured for hpMg (see right-hand axis in Fig. 8) also behaves in a similar manner as the one for cpMg (see Fig. 7). Both ER curves start with an increase, followed by a decrease at around 450 K. At higher temperatures a re-increase appears up to around 500 K and finally the ER curve decreases.

It should be pointed out that absolute values of ER plotted in Figs. 7 and 8 should be considered with care. Even if they are in reasonable agreement with the values reported for pure magnesium, 42 μΩ mm [26, 27], the length to diameter ratio of the samples is smaller than 5. In fact, the ER value is sensitive to the length of the sample when the length/diameter ratio is smaller than 5 [28]. However, we pay attention to the relative variation of ER instead of the absolute value.

4 Discussion

The homogenised sample measured in Fig. 3a, during the first heating run, shows a peak in the damping spectrum at 320 K. This peak was already reported for hpMg to be metastable and difficult to reproduce

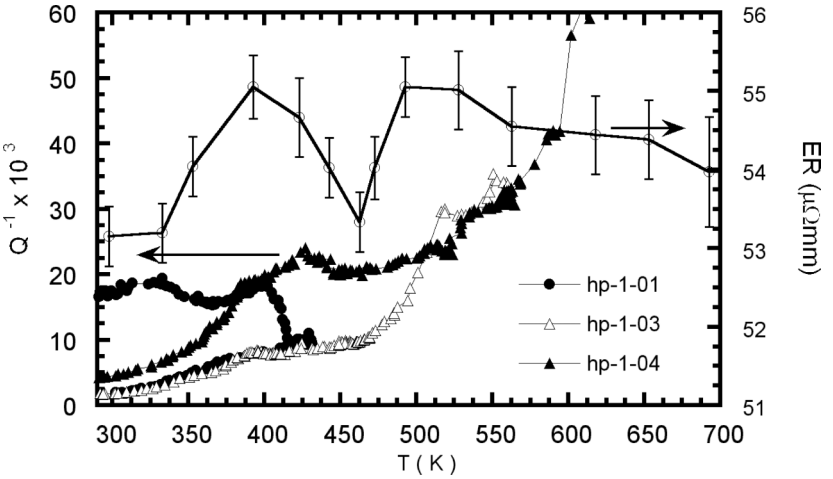

Fig. 8 Electrical resistivity in high-purity magnesium measured at room temperature as a function of the annealing temperature (empty circles). Damping measured in high-purity magnesium during different thermal cycles (as indicated in the legend).

[4]. The physical mechanism controlling this peak is still unclear, but this lack of information does not obstruct the subsequent analysis of the present work.

The damping plateau between 350 and 400 K during run-up #1 in Fig. 3a reveals the occurrence of some kind of interaction process between dislocations and point defects. In addition, the lack of appearance of the characteristic grain boundary damping peak indicates that the mobility of grain boundaries is strongly reduced. It is well known that the characteristic grain-boundary peak in unalloyed magnesium appears at around 420 K at a frequency of about 1 Hz [1–5]. In addition, we reported previously that grain-boundary relaxation can be inhibited by substitutional atoms that lock the movement of boundaries. In fact, in AZ91 and QE22 magnesium alloys the characteristic grain-boundary peak appears at temperatures between 420 and 450 K at 1 Hz, during the depletion of solute atoms from the supersaturated solid solution by the occurrence of precipitates [2, 3].

Nevertheless, grain-boundary locking by impurities should not be expected for the concentration of the cpMg samples employed in this work (see Table 1) [4, 7]. Consequently, the lack of a grain-boundary peak could be related to some kind of intrinsic locking of this relaxation. This point will be discussed in the followings paragraphs.

A damping decrease at around 420 K for the same kind of magnesium samples was earlier obtained in samples measured at RT by an isochronal annealing mode [6], in agreement with the present results. This damping decrease was assumed to be controlled by an impurity diffusivity increase with temperature produced by quenching or plastic deformation, out of thermodynamic equilibrium. This movement of impurities leads to the pinning of dislocations, producing a decrease of damping. In contrast, a decrease of point defect density at dislocations with increasing annealing temperature was assumed to be responsible for the re-increase of damping [6].

The elastic modulus behaviour plotted in Fig. 3c is in agreement with changes in the degree of mobility of dislocations and grain boundaries. In fact, the modulus increases after the first heating and remains higher during thermal cycles up to temperatures below 500 K. This is in agreement with the reduction of the damping background at low temperatures, close to room temperature, due to the decrease of dislocation mobility [29] (Fig. 3a and b). In addition, a higher elastic modulus within the temperature range of the grain-boundary relaxation for magnesium (400–550 K) can also be related to the grain boundary mobility decrease [1–3, 7, 16, 30–32]. Therefore, within this temperature range, the reduction of dislocation and grain-boundary mobility is occurring overlapped.

Subsequently, on increasing the final temperature of the thermal cycles above 500 K, the elastic modulus begins to decrease, reaching smaller values than for run-up #1. This indicates that dislocations and grain boundaries became more mobile, in agreement with both the increase of the background in the whole temperature range and the appearance of the grain-boundary relaxation (see curves 1-08-600 K and 1-12-690 K in Fig. 3a).

Therefore, in the temperature range between RT and about 500 K dislocations and grain-boundary mobility decrease in the homogenised samples. It will be shown in the following paragraphs that the degree of dislocation and grain-boundary mobility is controlled by the vacancy concentration in the matrix.

It is important to mention that there exists a controversy on the grain-boundary relaxation. Some authors pointed out that the relaxation is controlled by the sliding of dislocations, instead of grain-boundary sliding [4]. In fact, in the case of magnesium the characteristic grain-boundary relaxation was also related to dislocation glide controlled by jog climb and vacancy diffusion with an activation energy close to 100 kJ/mol (1.04 eV) [4, 33]. Nevertheless, this point is under open discussion; see for example Refs. [4, 7]. Hereafter, we refer to grain-boundary relaxation as grain-boundary relaxation itself or as dislocation relaxation at grain boundaries, because this point does not obstruct the subsequent analysis.

On the other hand, a creep-effect contribution to the damping peaks during the thermal cycles, at high temperatures, was eliminated after damping background subtraction. In fact, from about $0.4T_m$ the continuous increase of damping at high temperature follows a law approximately exponential with reciprocal temperature, the so-called high-temperature background [4, 7, 34], and is related to creep mechanisms [34].

As was shown in the preceding section (Fig. 6), the activation energy calculated for the peak at low temperature is 106 kJ/mol (1.11 eV). This value is not too far from the one of self-diffusion in magnesium (134 kJ/mol (1.4 eV) [24, 25]). In addition, the peak temperature is in good agreement with the peak temperature for the characteristic grain-boundary relaxation of magnesium [1–5, 7]. Therefore, it is reasonable to relate the peak at 420 K to the characteristic grain-boundary peak of magnesium. Consequently, this peak will be called hereafter the grain-boundary peak. Moreover, the constant peak height of deconvoluted grain boundary peaks during the thermal cycles, once they have developed and stabilised (see spectra 1-08-600 K and 1-12-690 K in Fig. 5a), supports the assumption made.

On the other hand, the activation energy calculated for the damping peak at about 490 K is 56 kJ/mol (0.59 eV). This small value indicates that this peak cannot be related to the solute grain boundary peak nor to the peak related to particles at grain boundaries in magnesium [1]. It is interesting to note that the calculated activation energy of 56 kJ/mol (0.59 eV) is close to the values of both vacancy formation and migration energies. In fact, the activation energy for vacancy migration is between 38 and 76 kJ/mol (0.4 and 0.8 eV) [24]. Besides, the activation energy for vacancy formation is between 55 and 85 kJ/mol (0.58 and 0.9 eV) [24, 35–43].

This peak develops after annealing the homogenised or deformed samples at temperatures over 500 K and it has a peak temperature within the interval of grain boundary relaxation peaks (400–550 K). In addition, the peak height increases in the deformed sample, Fig. 5b. Indeed, the damping peak height for a previously homogenised sample (1-06-570 K) is smaller than for a plastically deformed (2-03-550 K) one. We are comparing these two spectra, because both of them were annealed in the previous heating run, up to the same maximum temperature, 540 K, see Table 2. In addition, optical microscopy studies do not detect any grain-size change after the tests detailed in Table 2. Consequently, taking into account these facts and the activation energy found for the peak, we can relate this peak to a mechanism of interaction of free dislocations with vacancies. Besides, the positron average lifetime has also increased to 236.6 ps in the deformed sample, which is also in agreement with the proposed mechanism about the interaction of dislocations with vacancies. However, an interaction mechanism between vacancies, grain boundaries and free dislocations in the grain boundaries also could occur. Then, we refer to this peak as a damping peak involving vacancy interactions and it will be called hereafter a vacancy peak.

It is convenient to point out that the vacancy peak we are considering involves free dislocations. So, the increase in temperature after the last run-up (1-12-690 K) leads to a slight decrease in the dislocation density, but as indicated by the increase in the background values the quantity of dislocations which are free to move, owing to the temperature increase, is larger.

In agreement with the interaction mechanism involving vacancies in the present work, the appearance of a damping peak related to the interaction of vacancies with dislocations at temperatures of about $0.3T_m$ in high-purity single-crystalline molybdenum [44, 45] has been recently reported.

The peak height increase of the vacancy peak during the successive run-ups in temperature, Fig. 5a, can be explained considering dislocation and/or grain-boundary movement assisted by vacancy movement or formation. The increase in temperature leads to a larger quantity of vacancies allowing dislocations and/or grain boundaries to move, giving rise to the appearance of the grain-boundary and the vacancy peaks. A larger increase in the annealing temperature during the thermal cycles leads to a larger quantity of vacancies and consequently to a larger quantity of unlocked grain boundaries and dislocations, leading to their increase in the peak height. This mechanism is in agreement with the increase of the background values as the final temperature of the thermal cycles increases (see Fig. 3a) and with the decrease in moduli values (Fig. 3c).

Consequently, the movement of grain boundaries or dislocations would be assisted by the formation and diffusion of vacancies. This mechanism can be considered as the movement of the grain boundaries or dislocations in a viscous medium in a similar mode as was already proposed by Schoeck [46] for dislocations.

The ER curve in Fig. 7 increases, after the homogenisation treatment, up to about 350 K, which could be related to the development of internal stresses produced by thermally assisted movement of point defects (impurities and vacancies) out of thermodynamic equilibrium. It is in agreement with (a) the damping plateau and (b) the lack of appearance of the grain-boundary peak.

The decrease of the ER curve at 400 K could be related to the migration of impurities to vacancies, which is in agreement with the decrease in the average lifetime measured by PAS; see the right-hand axis in Fig. 7. In addition, both vacancies and impurities could also migrate to dislocations and grain boundaries with a similar effect on PAS and ER responses [10, 12].

A decrease in the damping values also appears at approximately the same temperature (420 K). Therefore, the jump down in the damping and the non-appearance of the grain-boundary peak could be related to the dislocations and grain boundary mobility decrease produced by the vacancy concentration reduction. This reduction could be produced by both the migration of impurities to vacancies and by the absorption of vacancies at dislocations and grain boundaries.

Increasing the temperature up to 500 K does not increase the vacancy concentration, as is indicated in Fig. 7, in agreement with the increase of the ER. The MS behaviour shows that the structure is still stressed for annealing temperatures up to around 500 K, as we mentioned before. The decrease in the elastic modulus and the appearance of the grain-boundary peak after thermal cycles up to about 540 K (see Fig. 3a and c) indicate that the recovery of internal stresses is more developed, in agreement with the behaviours of ER and PAS plotted in Fig. 7.

At temperatures higher than 500 K, the PAS curve increases slightly, as could be expected, and the ER curve decreases due to the decrease of the internal stresses promoted by vacancy-assisted mobility of defects within this temperature range. This is in agreement with the restoring of the grain-boundary peak and the decrease of the values of the elastic modulus, caused by the unlocking of grain boundaries and dislocations.

Therefore, it could be proposed that the damping decrease, at around 420 K, in the homogenised sample is related to the decrease of the vacancy density excess attained from the homogenisation treatment; both by impurity migration and/or by vacancy absorption during grain-boundary and dislocation movement, as a coupled physical mechanism. In fact, the decrease in the vacancy concentration reduces the possibility of dislocations and grain boundary movement within the temperature range RT–500 K, leading to the non-appearance of the characteristic grain-boundary peak and stressing the microstructure. During the successive heating runs over 500 K, the increase of vacancy content with increasing temperature allows more dislocations and/or grain boundaries to move. This will produce the re-arrangement of the microstructure recovering the internal stresses and leading to the appearance of the grain-boundary peak and the increase of the vacancy peak.

In another light, Fig. 8 shows that for a hpMg sample the temperatures where changes in the ER curve appear are in good agreement with the reported ones for cpMg. Therefore, a straightforward analysis leads us to propose that the first increase in the ER curve is related to an internal stresses increase. The ER decrease that follows the previous increase in the hpMg sample (see Fig. 8) should be related to a vacancy concentration reduction at these temperatures. The reduction is caused by grain-boundary and dislocation absorption due to the smaller concentration of impurity atoms in these samples. The next re-increase of ER can be related to both new vacancy generation and increase of internal stresses. Finally, the last decrease in ER is related to internal stresses reduction caused by the movement of grain boundaries and dislocations, assisted by the new vacancies.

The impurity content in hpMg is much smaller than in cpMg. Therefore, the role of impurities in hpMg for the reduction of grain-boundary and dislocation mobility cannot be very important. In fact, the decrease of the mobility of grain boundaries and dislocations is an intrinsic mechanism related to the absorption of vacancies during their movement after quenching. Indeed, the largest vacancy concentration reduction is observed between 420 and 500 K. Unlocking both grain boundaries and dislocations requires new vacancies, generated at higher temperatures over 500 K. Therefore, it can be established that effectively grain-boundary mobility in magnesium is controlled by vacancy concentration.

5 Conclusions

The grain-boundary relaxation and consequently the grain mobility in magnesium are developed through the absorption of vacancies. After quenching from 823 K, the vacancies in excess are consumed at

420 K, locking grain boundaries and dislocations. New vacancies generated by heating at temperatures over 500 K are required for unpinning dislocation and grain-boundary structures.

Electrical resistivity and positron lifetime spectroscopy together with mechanical spectroscopy have been found to be very appropriate techniques to follow the evolution of the microstructure in commercial pure and high-purity magnesium.

A new damping peak related to vacancies in magnesium at 490 K, having an activation energy of 56 kJ/mol (0.59 eV), has been observed.

Acknowledgements We acknowledge Prof. P. Lukáč for Refs. [32–40] and for stimulating discussions, C. E. Bortolotto for his collaboration in obtaining some experimental data and Milos Janecek for carrying out the TEM work. This work was partially supported by the Collaboration Agreement between the University of the Basque Country and the Universidad Nacional de Rosario (UPV224.310-14553/02 and Res. CS. 788/88–1792/2003), the Collaboration Agreement between the Clausthal University of Technology and the Universidad Nacional de Rosario (Res. CS. 2702/2006), the PEI-CONICET Nos. 6206 and 5665, the UNR-PID 2003/2004 and 2005/2007 and the EIE, FCEIA and UNR.

References

[1] O. A. Lambri, W. Riehemann, L. M. Salvatierra, and J. A. García, Mater. Sci. Eng. A **373**, 146 (2004).
[2] O. A. Lambri, W. Riehemann, and Z. Trojanová, Scr. Mater. **45**, 1365 (2001).
[3] O. A. Lambri and W. Riehemann, Scr. Mater. **52**, 93 (2005).
[4] R. Schaller, G. Fantozzi, and G. Gremaud (eds.), Mechanical Spectroscopy (Trans Tech, Switzerland, 2001).
[5] T. S. Ké, Phys. Rev. **71**, 533 (1947).
[6] W. Riehemann and F. Abed El-Al, J. Alloys Compd. **310**, 127 (2000).
[7] A. S. Nowick and B. S. Berry, Anelastic Relaxation in Crystalline Solids (Academic Press, New York, 1972).
[8] J. S. Dugdale, The Electrical Properties of Metals and Alloys (Arnold, London, 1977).
[9] J. A. Delaney and A. B. Pippard, Rep. Prog. Phys. **35**, 677 (1972).
[10] W. Brandt and A. Dupasquier (eds.), Positron Solid-State Physics (North-Holland, Amsterdam, 1983).
[11] J. M. Campillo and F. Plazaola, Defect Diffus. Forum **213–215**, 141 (2003).
[12] M. J. Puska and R. M. Nieminen, Rev. Mod. Phys. **66**, 841 (1994).
[13] A. Dupasquier, G. Kögel, and A. Somoza, Acta Mater. **52**, 4707 (2004).
[14] M. Eldrup, Application of the positron annihilation technique in studies of defects in solids, in: Defects in Solids, edited by A. V. Chadwick and M. Terenzi, NATO ASI Ser. (Plenum Press, New York, 1986).
[15] P. Hautojärvi, J. Johansson, A. Vehanen, and J. Yli-Kauppila, Appl. Phys. A **27**, 49 (1982).
[16] F. J. Humphreys and M. Hatherly, Recrystallization and Related Annealing Phenomena (Pergamon/Elsevier Science, The Netherlands, 2002).
[17] O. A. Lambri, Mater. Trans. JIM **35**, 458 (1994).
[18] O. A. Lambri, A review on the problem of measuring non-linear damping and the obtainment of intrinsic damping, in: Materials Instabilities, edited by J. Martinez-Mardones, D. Walgraef, and C. H. Wörner (World Scientific, Singapore, New Jersey, 2000), p. 249.
[19] J. A. García, S. Hull, S. Messoloras, and R. J. Stewart, J. Phys. E, Sci. Instrum. **21**, 466 (1988).
[20] P. Kirkegaard, N. J. Pedersen, and M. Eldrup, PATFIT-88 program, Tech. Rep. No. M-2740 (Riso National Laboratory, Roskilde, Denmark, 1989).
[21] I. MacKenzie, Positron Solid State Physics, Proc. 83rd Int. "Enrico Fermi" School of Physics, edited by W. Brandt and A. Dupasquier (North-Holland, Amsterdam, 1983), p. 210.
[22] R. T. C. Tsui, Acta Metall. **15**, 1723 (1967).
[23] Peak Fit V.4 (Jandel Scientific Software, Germany, 1996).
[24] H. Ullmaier (ed.), Landolt-Börnstein, Crystal and Solid State Physics, Vol. 25, Atomic Point Defects in Metals (Springer-Verlag, Berlin, 1991).
[25] P. G. Schewmon, Trans. Am. Inst. Mineral. (Metall.) Eng. **206**, 918 (1956).
[26] M. M. Avedesian and H. Baker (eds.), ASM Specialty Handbook, Magnesium and Magnesium Alloys (ASM International, The Materials Information Society, Cleveland, Ohio, 1999).
[27] E. A. Brandes and G. B. Brook (eds.), Smithells Metals Ref. Book (Butterworth Heinemann, Oxford, 1999).
[28] J. LePage, A. Bernalte, and D. A. Lindholm, Rev. Sci. Instrum. **39**, 1019 (1968).

[29] A. Granato and K. Lücke, J. Appl. Phys. **27**, 583 (1956).
[30] R. B. Nicholson, in: Strong Microstructures from the Solid State in Phase Transformations, edited by H. I. Aaronson (ASM, Cleveland, Ohio, 1970), p. 550.
[31] G. Gottstein and L. S. Shvindlerman, Grain Boundary Migration in Metals: Thermodynamics, Kinetics, Applications (CRC Press, New York, 1999).
[32] R. W. Cahn and P. Haasen, Physical Metallurgy (North-Holland, Amsterdam, 1983).
[33] C. Esnouf and G. Fantozzi, J. Phys. (Paris) **42**, C5-445 (1981).
[34] J. Friedel, Dislocations (Addison-Wesley, Reading, MA, 1967).
[35] C. Janot, D. Malejse, and B. George, Phys. Rev. B **2**, 3088 (1970).
[36] J. J. Beevers, Acta Metall. **11**, 1029 (1963).
[37] P. Tzanetakis, J. Hillairet, and G. Revel, phys. stat. sol. (b) **75**, 433 (1976).
[38] J. S. Koehler, F. Seitz, and J. E. Bauerle, Phys. Rev. **107**, 1499 (1957).
[39] M. Manninen and R. Nieminen, J. Phys. F **8**, 22243 (1978).
[40] M. Manninen, Phys. Rev. B **12**, 4012 (1975).
[41] T. Mori, M. Meshii, and J. Kauman, J. Appl. Phys. **33**, 2775 (1962).
[42] A. Seeger and E. Mann, J. Phys. Chem. Solids **12**, 326 (1960).
[43] H. K. Sahu, S. Srinivasa, and K. Kirshan, Radiat. Eff. Lett. **50**, 72 (1980).
[44] O. A. Lambri, G. I. Zelada-Lambri, L. M. Salvatierra, J. A. García, and J. N. Lomer, Mater. Sci. Eng. A **370**, 222 (2004).
[45] G. I. Zelada-Lambri, O. A. Lambri, and J. A. García, J. Nucl. Mater. **353**, 127 (2006).
[46] G. Schoeck, phys. stat. sol. (a) **32**, 651 (1969).

